PCCP

PAPER

View Article Online
View Journal | View Issue

Cite this: *Phys. Chem. Chem. Phys.*, 2016, **18**, 15719

Blue-shifted emission and enhanced quantum efficiency *via* π-bridge elongation in carbazole–carborane dyads†

Zhaojin Wang,[a] Peng Jiang,[a] Tianyu Wang,[a] Graeme J. Moxey,[b] Marie P. Cifuentes,[ab] Chi Zhang*[a] and Mark G. Humphrey*[ab]

Received 29th April 2016,
Accepted 20th May 2016

DOI: 10.1039/c6cp02870e

www.rsc.org/pccp

Carbazole–carborane linear dyads and di(carbazole)–carborane V-shaped dyads with phenyleneethynylene-based bridges have been synthesized. The V-shaped dyads display the expected red-shifts in the location of their UV-Vis absorption maxima on bridge-lengthening, but show unusual blue-shifts in charge-transfer (CT) emission on the same π-system lengthening. These blue-shifts can be attributed to the $2n + 3$ electron count within the carborane cluster in the excited state. The linear dyads luminesce *via* a combination of local excited (LE) and CT emission, with a red-shift in LE emission and a blue-shift in CT emission accompanying π-bridge elongation. A quantum efficiency as high as 86% in the solution state is achieved from the hybrid LE/CT emission. Time-dependent density functional theory (TD-DFT) calculations at the excited state of these compounds have clarified the photoluminescence blue-shift and suggested a typical cluster C–C bond elongation in the V-shaped dyads. Calculations on the elongated linear dyads have suggested that the electron density is localized at the phenyleneethynylene-containing bridge.

Introduction

The last two decades have witnessed wide-ranging applications of electron donor–acceptor (D–A) dyads in the fields of photovoltaics,[1] electronics, and light-emitting diodes.[2] The pursuit of improved dyads has resulted in the study of a large number of donors, but the range of acceptors investigated is still limited.[3] One promising candidate as an acceptor, *o*-carborane (*o*-Cb, $C_2B_{10}H_{12}$) has attracted considerable attention recently,[4] not only because of its strong electron deficiency,[4b,j,5] but also because of its three-dimensional pseudo-aromaticity, high thermal stability, and bio-compatibility, which give this novel acceptor several advantages as a key module in the design of new materials.[2g,6]

Many *o*-Cb dyads have been reported, and their photoluminescence (PL) properties have been studied extensively (the majority are in fact *o*-Cb triads with two identical donors).[7] *o*-Cb dyads usually exhibit emission that is predominantly charge-transfer (CT) in nature, with large Stokes shifts, intensities that are solvent-dependent, relatively low efficiencies, and quenching in polar solvents. In contrast to their solution behaviour, *o*-Cb dyads experience a significant enhancement in intensity on proceeding to the solid state, due to aggregation-induced emission (AIE)[8] and, in one case, crystal-induced emission (CIE).[9] In the neat film state, recently reported *o*-Cb triad assemblies with electron donor and acceptor groups have also exhibited excellent thermally activated delayed fluorescence (TADF) in addition to AIE, with quantum efficiencies up to 97%.[10] Nevertheless, with minimal exceptions,[11] studies of *o*-Cb dyads have focused on compounds with small π-systems, as the scope of the linkages within the *o*-Cb dyads has thus far been confined to a phenylene unit; in particular, efforts to adjust or improve the PL are limited to substituent variation. In view of the enormous importance of the π-bridge in electron transfer,[12] we reasoned that oligo(phenylene-ethynylene) units may prove beneficial bridges connecting di-*tert*-butylcarbazole donor(s) (^Cz, D) and *o*-carborane acceptor (*o*-Cb, A) and herein report six *o*-Cb dyads (**D-1**/**D-2**/**D-3**, **M-1**/**M-2**/**M-3**, Scheme 1), together with the unusual trend in their PL properties that is seen on π-bridge extension.

Results and discussion

V-shaped dyads **D-1**/**D-2**/**D-3** and linear dyads **M-1**/**M-2**/**M-3** were synthesized as described in the experimental section and characterized by the usual spectroscopies and a single-crystal X-ray

[a] *School of Chemical and Material Engineering, Jiangnan University, Wuxi 214122, Jiangsu Province, China. E-mail: mark.humphrey@jiangnan.edu.cn*
[b] *Research School of Chemistry, Australian National University, Canberra, ACT 2601, Australia. E-mail: Mark.Humphrey@anu.edu.au*

† Electronic supplementary information (ESI) available: NMR spectra, crystallographic procedures, photophysical studies, Cartesian coordinates and energies of DFT optimized structures. CCDC 1457766. For ESI and crystallographic data in CIF or other electronic format see DOI: 10.1039/c6cp02870e

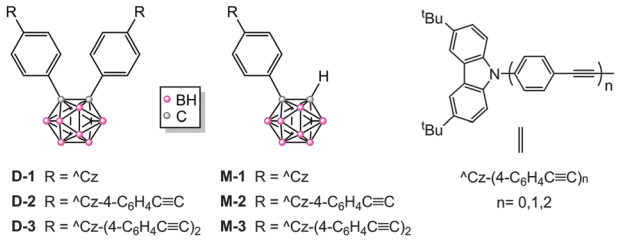

Scheme 1 Structures of the *o*-Cb dyads.

diffraction study of **D-3** (Fig. 1). Fig. 2 shows the linear optical absorption spectra of these *o*-Cb dyads. The same variation in spectra on π-bridge elongation is observed for the V-shaped (**D**) and linear (**M**) sets of dyads. Excluding the constant absorption at *ca.* 295 nm, the *o*-Cb dyads display similar red-shifts in bands corresponding to the same type of electronic excitation. For example, the absorption corresponding to one $\pi_{\text{^CzB}}$–$\pi_{\text{^CzB}}^*$ transition (B = bridge) appears at 331 nm for **D-1**,[13] 347 nm for **D-2**, and 348 nm for **D-3**, while the absorption for a further $\pi_{\text{^CzB}}$–π_{CbB}^* transition appears at 342 nm for **D-1**, 368 nm for **D-2**, and is further red-shifted for **D-3**.

The PL spectra of the V-shaped dyads were assessed following excitation at 350 nm (Fig. 3a–c). A blue-shift in the PL maximum is seen upon π-bridge elongation, in contrast to the red-shift seen with the absorption bands following the same bridge lengthening. In cyclohexane, the maximum emission peaks appear at 570 nm for **D-1**, 521 nm for **D-2**, and 496 nm for **D-3**, a blue-shift of 74 nm following incorporation of a di(phenylene-ethynylene) linkage. A similar variation was observed in carbon tetrachloride and toluene, with the emission shifting from 591 nm to 514 nm and from 632 nm to 563 nm under the same π-system lengthening, corresponding to a blue shift of 77 nm and 69 nm, respectively. This constant blue shift is not seen either in more polar solvents (because this CT emission is quenched, leaving only local excited (LE) emissions (Fig. 3d)) or in the solid state

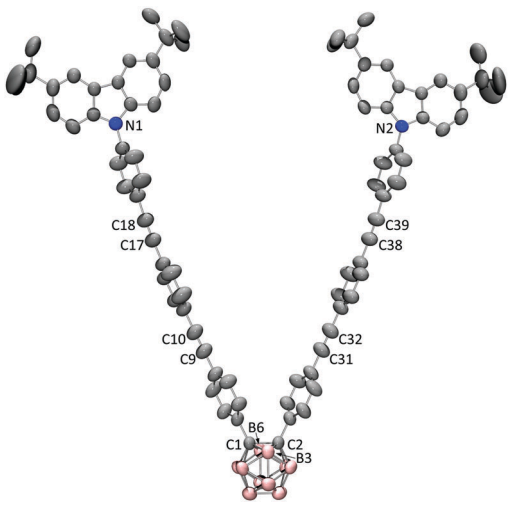

Fig. 1 Crystal structure of **D-3**. Selected bond lengths (Å): C1–C2 1.718(3), C9–C10 1.187(3), C17–C18 1.198(3), C31–C32 1.187(3), C38–C39 1.198(3), C1–N1 19.376, C2–N2 19.376. Hydrogen atoms have been omitted for clarity.

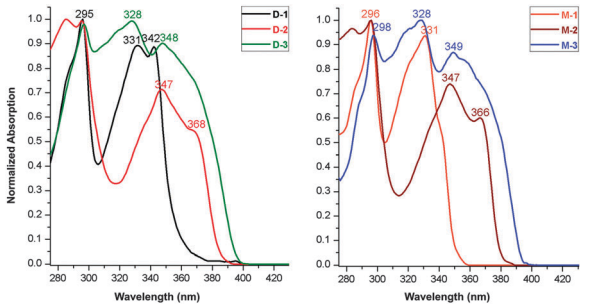

Fig. 2 Normalized absorption of **D-1**/**D-2**/**D-3** (left) and **M-1**/**M-2**/**M-3** (right) dyads in cyclohexane solvent.

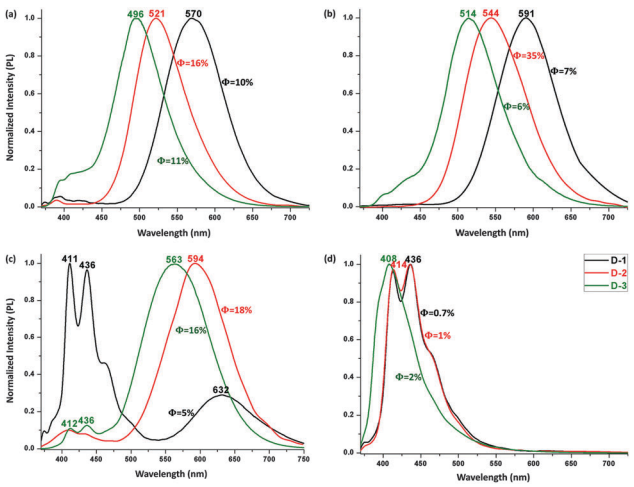

Fig. 3 Normalized PL spectra of **D-1**, **D-2** and **D-3** (2 μM) in c-C_6H_{12} (a), CCl_4 (b), toluene (c) and $CHCl_3$ (d), with excitation at 350 nm.

(because only a weak to moderate orange emission is seen, due to an aggregation-caused quenching (ACQ) effect). Among these V-shaped dyads, **D-2** is the most highly emissive, with quantum efficiencies (QE, Φ) 16–35% in the less polar solvents (Table S1 in ESI†).

The polyhedral skeletal electron pair theory (PSEPT) electron counting rules (Wade–Mingos rules) dictate that the *o*-Cb clusters are held together by 26 ($2n$ + 2, n = 12) skeletal electrons.[14] Ordinarily, one would expect that the HOMO would rise while the LUMO would fall in energy following π-bridge extension in such dyads, which together result in red shifts in the absorption bands. However, previous studies of the V-shaped *o*-Cb dyad **D-1** revealed the presence of a key excited state containing $Cz^{\bullet+}$ and $Cb^{\bullet-}$ and a typical carboranyl C–C bond cleavage,[13] and thus the origin of PL is actually the charge-separated $Cz^{\bullet+}$–π–$Cb^{\bullet-}$. The electron-counting of the *o*-Cb cluster is therefore $2n$ + 3 in this case, and the electronic properties of both Cz and Cb are inverted relative to their initial properties. The energetic trend in HOMO (located at ^Cz) and LUMO (located at *o*-Cb) is therefore reversed following π-extension, the HOMO falling and the LUMO rising in energy, resulting in the observed blue-shift in PL. We anticipate that the PL behaviour of other *o*-Cb dyads can be tuned in a

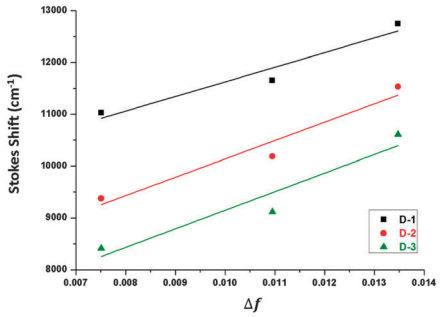

Fig. 4 Mataga–Lippert plots for CT emissions of **D-1**, **D-2** and **D-3**.

similar fashion, as is corroborated by two oligo(phenylene) linked examples.[13]

Fig. 4 shows Mataga–Lippert plots for the solvatochromic shifts of the CT emission of the V-shaped dyads and the estimation of the dipole moment was empirically following the Mataga–Lippert equation, expressed as follows:

$$V_a - V_f = \frac{2(\mu_e - \mu_g)^2}{hca^3}\Delta f, \quad \Delta f = \left(\frac{\varepsilon - 1}{2\varepsilon + 1} - \frac{n^2 - 1}{2n^2 + 1}\right)$$

where μ_e and μ_g are the dipole moments in the excited and ground states, respectively, c is the velocity of light, h is Plank's constant, and a is the radius of the Onsager cavity around the fluorophore. The solvent dielectric constant (ε) and refraction index (n) are included in the term, Δf. The dipole moments in the excited states are *ca.* 35 D for **D-1**, 92 D for **D-2** and 169 D for **D-3** (Table S2 in ESI†). Though the values are likely overestimated for **D-2** and **D-3**, a strong increase in dipole moment is clearly present, correlating with the afore-mentioned charge-separated excited state and the increasing distance between the ^Cz and *o*-Cb moieties.

To verify the general nature of this unusual blue-shift, we examined the linear dyads, **M-1**/**M-2**/**M-3**, which possess more complicated PL due to dual emission.[13b] Fig. 5a shows the emission spectra in which the LE band (<450 nm) and the CT band (>450 nm) are broad and possess large Stokes shifts. The LE band shows a slight red-shift of 9 nm in proceeding from **M-1** to **M-2** whereas the CT band shows a blue-shift of 42 nm. This variation continues on proceeding to **M-3**, affording a band with both LE and CT character (Fig. S2.2(f) in ESI†). The relative intensities of the LE and CT emissions vary upon π-bridge elongation (LE : CT intensity ratios 1 : 10 (**M-1**), 1 : 1.5 (**M-2**), 1 : ≈0 (**M-3**)). More importantly, the harvested QE increases significantly on π-extension; for example, the QE of **M-3** is 86% in c-C_6H_{12} and 85% in toluene, the highest values for emissive *o*-Cb derivatives in the solution state,[7f,15] while the QEs for **M-2** and **M-1** are much lower. The linear dyads exhibit emission quenching in the more polar solvents, **M-3** harvesting only 2% QE in THF (Table S1 in ESI†). Study of the PL in the solid state showed that **M-3** possesses a weak blue emission while the other linear compounds show weak multiplex emission.

Within an individual linear dyad, there is a clear-cut progression from LE to CT emission, as can be seen in the PL spectra of **M-2** in Fig. 5b. The higher energy peak corresponds to LE emission (LE′)

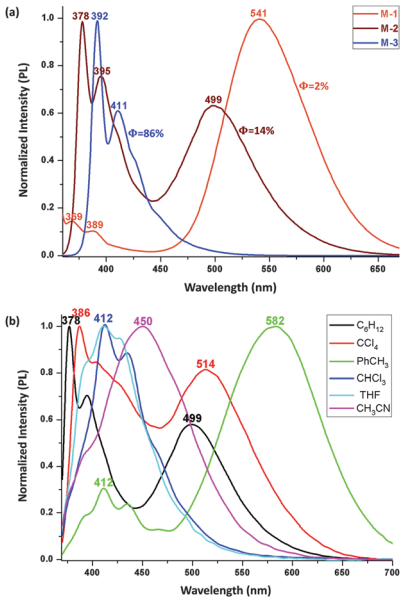

Fig. 5 (a) Normalized PL of **M-1** (20 μM), **M-2** and **M-3** (2 μM) in C_6H_{12}; (b) normalized PL of **M-2** (2 μM) in different solvents, both were excited at 350 nm.

and the lower energy peak to CT, so the energy difference between the LE′ and CT maxima is *ca.* 0.797 eV in c-C_6H_{12}, *ca.* 0.802 eV in CCl_4, *ca.* 0.880 eV in toluene, and even larger in more polar solvents as the CT state decreases in energy faster than the LE′ state (Table 1). Once a threshold for quenching is met, the larger stabilization results in a change in character of the emission from LE to CT and dramatic quenching, not only in CT but also in LE, until no QE is harvested for all *o*-Cb dyads. In other words, although the linear dyads exhibit both LE and CT emission, the progression from LE to CT emission (that may be accompanied by C–C bond cleavage) will inevitably lead to an overall loss in PL intensity. The π-bridge elongation on proceeding to **M-3** reduces this comparative stabilization of CT *vs.* LE. These results also suggest that by changing the electron donor, one should be able to influence the relative LE and CT emissions, and thereby tune the PL in a relatively simple fashion.

To better understand the unusual properties of these π-bridge-elongated *o*-Cb dyads, time-dependent density-functional theory (TD-DFT) calculations were performed at the (u)M06-2X[16]/6-31G(d,p) level. The calculated electronic transitions for all the *o*-Cb dyads in their ground states are in good agreement with the red-shift in their homogeneous absorption bands (Table S3, ESI†). Moreover, the experimentally-observed blue shift in PL is also verified in the emission modelling of the V-shaped *o*-Cb dyads. Fig. 6 shows the calculated electronic transitions of **D-1** and **D-2** at the first singlet excited state (S_1). The optimized geometries of

Table 1 Variation in energies of the LE and CT states for **M-2** as the solvent is varied

Energy (eV)	c-C_6H_{12}	CCl_4	$PhCH_3$	$CHCl_3$
LE′	3.287	3.219	3.015	3.015
CT	2.490	2.417	2.135	—
ΔE (eV)	0.797	0.802	0.880	—

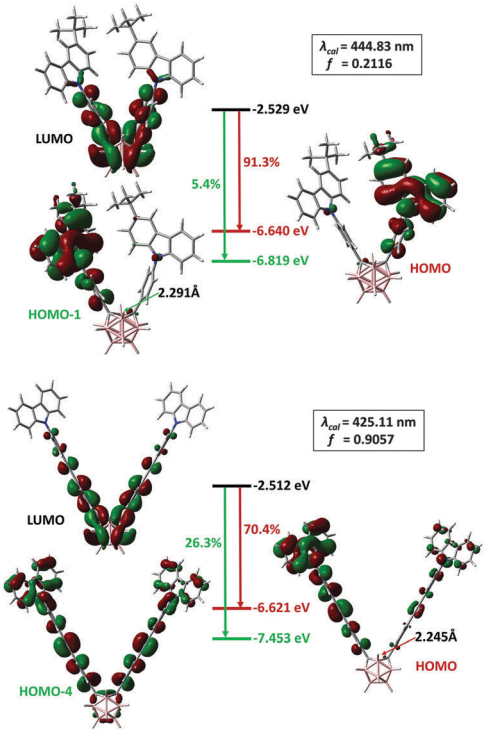

Fig. 6 Emission simulations of **D-1** (top) and **D-2** (bottom). The carboranyl C···C distance is listed in Å and the assignment of the electronic transitions is shown as a percentage.

the S_1 state contain characteristic carboranyl C···C distances of 2.291 Å for **D-1** and 2.245 Å for **D-2**, in accordance with reported values.[17] Such elongated C–C bonds are characteristic of *o*-Cb anions with $2n + 3$ skeletal electrons.[17b] The calculated wavelengths, 444.83 nm for **D-1** and 425.11 nm for **D-2**, along with the oscillator strengths (f) 0.2117 and 0.9057, respectively, are in agreement with the observed blue-shift if one neglects the underestimation due to the high content of Hartree–Fock exchange (54%) within the M06-2X functional.[16] The HOMO–LUMO gap does not change significantly; the blue shift in proceeding from **D-1** to **D-2** can therefore be attributed to greater participation of transitions from the LUMO to orbitals lower than the HOMO (for example, the 26.3% contribution from LUMO to HOMO−4).

The emission modelling of **M-3** at the S_1 state revealed a strong bias towards LE emission (Fig. S3.12 in the ESI†), supported in two ways. Firstly, the S_1 geometry is similar to that of the ground state S_0 with only a slightly longer carboranyl C–C bond (difference *ca.* 0.027 Å: the comparable value in **D-2** is 0.562 Å). Secondly, the LUMO at the S_1 state is mostly located on the π-bridge (Fig. 7c) with only a *ca.* 2.9% contribution from *o*-Cb, and therefore comparable to that of the S_0 state. To evaluate the possible CT emission in **M-3**, modelling on the one-electron-imposed state (an imaginary anion to mimic the LUMO at the S_1 state: Fig. 7b) was undertaken; this revealed a similar distribution in the highest singly occupied molecular orbital (HSOMO at the DFT level), for which the contribution from *o*-Cb is only 4.1%, consistent with resemblance between the S_1 states for LE and CT emission. Such a hybrid excited state agrees with the observed

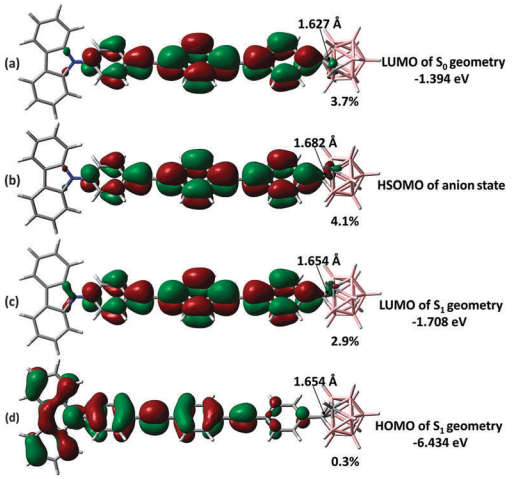

Fig. 7 Selected frontier orbitals of **M-3** for different states. The carboranyl C–C bond length is listed in Å and the *o*-Cb contribution to each orbital is shown as a percentage.

LE-predominant emission, the CT character in more polar solvents, and the LE to CT transformation.

By consulting both the LUMO of **D-3** (Fig. S3.9 in the ESI†) and **M-3** at the S_1 state structure, the cluster contribution which is in response to the electron withdrawing effect of *o*-Cb is overwhelming in the V-shaped **D-3** (58.8%) while it is actually inclined to the absence in the linear **M-3**. Therefore the photophysical properties of *o*-Cb dyads, especially those at their excited state, are strongly determined by the π-extending bridge, as well as the fashion of substitution.

Conclusions

In summary, π-bridge elongation has been shown to be a highly effective way to tune the photoluminescence of both V-shaped and linear *o*-Cb dyads and, in particular, a facile route to an extraordinary blue-shift in PL. The π-bridge elongation in the linear dyads also leads to a unique hybrid excited state, LE and CT emission, and very high PL efficiency. These outcomes can be attributed to the unique electronic structure of *o*-Cb in the corresponding excited states, as supported by the TD-DFT calculations. Our findings suggest that *o*-Cb dyads can be engineered to possess very large excited-state dipole moments, as in the V-shaped assemblies, and that emissive *o*-Cb dyads can be designed with specific PL properties, as in the linear constructions.

Experimental section

The preparative work was carried out under a nitrogen atmosphere using standard Schlenk techniques. Solvents were freshly distilled under nitrogen from either sodium or calcium hydride prior to use. Reactants 3,6-di-*tert*-butyl-9*H*-carbazole, 3,6-di-*tert*-butyl-9-(4-ethynylphenyl)-9*H*-carbazole, 3,6-di-*tert*-butyl-9-(4-((4-ethynylphenyl)ethynyl)phenyl)-9*H*-carbazole, (4-iodophenyl)-*o*-carborane and bis(4-iodophenyl)-*o*-carborane were prepared according to literature methods.[18] Other chemicals were used as commercial

products without further purification. Tetrakis(triphenylphosphine)palladium(0) (J&K) was 99.8% grade. The NMR data were obtained on a Bruker DRX 400 spectrometer; chemical shifts are given with respect to $CHCl_3/CDCl_3$ (δ ^{1}H = 7.24 ppm, δ ^{13}C = 77.00 ppm) and external $BF_3{\cdot}Et_2O$ (δ ^{11}B = 0 ppm). Mass spectral data were recorded on a Bruker Daltonics ultrafleXtreme MALDI-TOF/TOF, Micromass/Waters LCT-ZMD single quadrupole liquid chromatograph-MS or a VG Quattro II triple quadrupole MS. Elemental analyses were performed on Elementar vario MICRO cube (Germany). The absorption and photoluminescence spectra were recorded on a UV-Vis-NIR spectrophotometer (Shimadzu UV-3600 plus) and a fluorescence spectrophotometer (Hitachi F-4600) equipped with high performance R928 photomultiplier detector.

Synthesis of M-1, M-2, M-3, D-1, D-2 and D-3

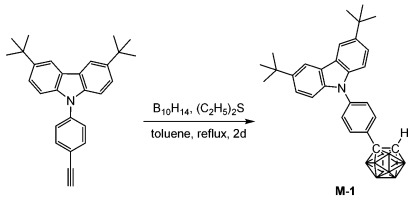

The synthesis of **M-1** followed the conventional method for the preparation of *o*-carborane derivatives using $B_{10}H_{14}$ as the precursor.[19] Heating 3,6-di-*tert*-butyl-9-(4-ethynylphenyl)-9*H*-carbazole (380 mg, 1.0 mmol), $B_{10}H_{14}$ (147 mg, 1.2 mmol) and diethyl sulfide (220 mg, 2.4 mmol) in refluxing anhydrous toluene for 2 days afforded **M-1** (273 mg, 55%) as a white powder after work-up. ^{1}H NMR (400 MHz, $CDCl_3$): δ (ppm) 8.12 (2H, s, Ar–H), 7.67 (2H, d, 8.5 Hz, Ar–H), 7.54 (2H, d, 8.5 Hz, Ar–H), 7.45 (2H, d, 8.5 Hz, Ar–H), 7.34 (2H, d, 8.5 Hz, Ar–H), 4.02 (1H, s, C_{carb}–H), 3.6–1.6 (10H, br, B–H), 1.45 (18H, s, CH_3); ^{13}C NMR (101 MHz, $CDCl_3$): δ (ppm) 143.59, 140.03, 138.55, 131.34, 129.22, 126.32, 123.80, 123.75, 116.41, 109.06 (18C, Ar–C), 76.04 (C_{carb}), 60.48 (C_{carb}), 34.75 (2C, CMe_3), 31.95 (6C, CH_3); ^{11}B NMR (128 MHz, $CDCl_3$): δ (ppm) −1.16 (1B), −2.33 (1B), −8.20 (2B), −9.43 (2B), −9.91 (2B), −11.27 (2B); MS (MALDI-TOF): *m*/*z* calcd for $C_{28}H_{39}B_{10}N$ 498.405 (100%), found for $C_{28}H_{39}B_{10}N$ 498.414 (100%). Anal. calcd for $C_{28}H_{39}B_{10}N$: C, 67.57; H, 7.90; N, 2.81. Found: C, 67.83; H, 8.13; N, 2.52.

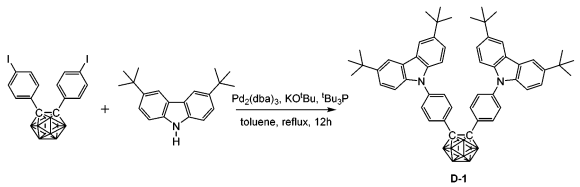

The synthesis of **D-1** proceeded *via* Buchwald–Hartwig coupling[20] of bis(4-iodophenyl)-*o*-carborane (548 mg, 1.0 mmol) and 3,6-di-*tert*-butyl-9*H*-carbazole (560 mg, 2.0 mmol), and using $Pd_2(dba)_3$ (19 mg, 0.02 mmol), ^{t}Bu$_3$P (260 μL, 10% in pentane, 0.08 mmol) and KO^{t}Bu (225 mg, 2.0 mmol) as catalysts or additives. The reaction mixture was heated in refluxing toluene for 12 h under a N_2 atmosphere. The crude product was purified by flash chromatography on silica gel using hexane as eluent, affording **D-1** (451 mg, 53%) as a white powder. ^{1}H NMR (400 MHz, $CDCl_3$): δ (ppm) 8.07 (4H, s, Ar–H), 7.65 (4H, d, 8.5 Hz, Ar–H), 7.42 (4H, d, 8.5 Hz, Ar–H), 7.23 (4H, d, 8.5 Hz, Ar–H), 7.18 (4H, d, 8.5 Hz, Ar–H), 3.92–1.97 (10H, br, B–H), 1.39 (36H, s, CH_3); ^{13}C NMR (101 MHz, $CDCl_3$): δ (ppm) 143.52, 140.28, 138.36, 132.16, 128.49, 125.67, 123.78, 123.76, 116.36, 108.87 (36C, Ar–C), 84.73 (2C, C_{carb}), 34.67 (4C, CMe_3), 31.91 (12C, CH_3); ^{11}B NMR (128 MHz, $CDCl_3$): δ (ppm) −2.13 (4B, br), −10.20 (6B, br); MS (MALDI-TOF): *m*/*z* calcd for $C_{54}H_{66}B_{10}N_2$ 851.620, found for $C_{54}H_{66}B_{10}N_2$ 851.620. Anal. calcd for $C_{54}H_{66}B_{10}N_2$: C, 76.19; H, 7.81; N, 3.29. Found: C, 75.93; H, 7.74; N, 3.16.

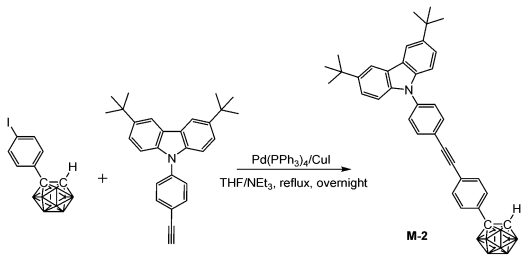

In a 100 mL Schlenk tube, a mixed solvent of THF/NEt_3 (20 mL/10 mL) was degassed by freeze–pump–thaw cycles and then frozen again using liquid nitrogen. After purging with a N_2 stream, (4-iodophenyl)-*o*-carborane (347 mg, 1.0 mmol), 3,6-di-*tert*-butyl-9-(4-ethynyl-phenyl)-9*H*-carbazole (380 mg, 1.0 mmol), $Pd(PPh_3)_4$ (35 mg, 0.03 mmol), and CuI (10 mg, 0.05 mmol) were added and the N_2 atmosphere was evacuated-backfilled twice. The reaction mixture was slowly warmed to room temperature and then refluxed overnight. After cooling and evaporation of the solvent, the crude product was purified by flash chromatography on silica gel using hexane/CH_2Cl_2 (v : v 10 : 1) as eluent. Recrystallization from a hot mixed solvent of hexane/CH_2Cl_2 (v/v, 3 : 1) gave **M-2** (482 mg, 81%). ^{1}H NMR (400 MHz, $CDCl_3$): δ (ppm) 8.14 (2H, s, Ar–H), 7.72 (2H, d, 8.5 Hz, Ar–H), 7.56 (2H, d, 8.5 Hz, Ar–H), 7.48 (6H, m, Ar–H), 7.38 (2H, d, 8.5 Hz, Ar–H), 3.93 (1H, s, C_{carb}–H), 3.4–1.6 (10H, br, B–H), 1.46 (18H, s, CH_3); ^{13}C NMR (101 MHz, $CDCl_3$): δ (ppm) 143.32, 138.76, 138.60, 133.18, 133.14, 131.83, 127.61, 126.36, 125.13, 123.75, 123.62, 120.82, 116.33, 109.15 (24C, Ar–C), 91.35, 88.40 (2C, C≡C), 75.96 (C_{carb}), 60.08 (C_{carb}), 34.75 (2C, CMe_3), 31.98 (6C, CH_3); ^{11}B NMR (128 MHz, $CDCl_3$): δ (ppm) −1.30 (1B), −2.49 (1B), −8.19 (2B), −9.41 (2B), −10.09 (2B), −11.38 (2B); MS (MALDI-TOF): *m*/*z* calcd for $C_{36}H_{43}B_{10}N$ 598.436, found for $C_{36}H_{43}B_{10}N$ 598.439; HRMS (EI): *m*/*z* calcd for $C_{36}H_{43}B_{10}N$ 598.4248 (100%), found for $C_{36}H_{43}B_{10}N$ 598.4252 (100%). Anal. calcd for $C_{36}H_{43}B_{10}N$: C, 72.32; H, 7.25; N, 2.34. Found: C, 71.96; H, 7.20; N, 2.28.

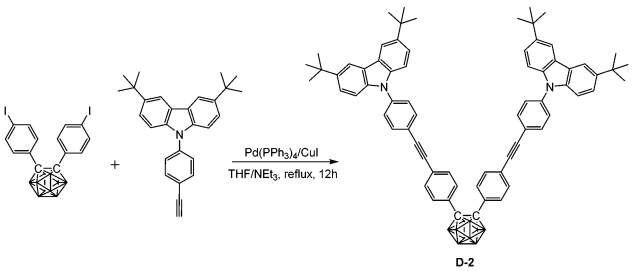

In a 100 mL Schlenk tube, a mixed solvent of THF/NEt_3 (15 mL/10 mL) was degassed by freeze–pump–thaw cycles and then frozen again using liquid nitrogen. After purging with a

N_2 stream, bis(4-iodophenyl)-*o*-carborane (548 mg, 1.0 mmol), 3,6-di-*tert*-butyl-9-(4-ethynylphenyl)-9*H*-carbazole (759 mg, 2.0 mmol), $Pd(PPh_3)_4$ (69 mg, 0.06 mmol), and CuI (12 mg, 0.06 mmol) were added and the N_2 atmosphere was evacuated-backfilled twice. The reaction mixture was gradually warmed to room temperature and afterwards refluxed for 12 h. After cooling and evaporation of the solvent, the crude product was purified by flash chromatography on silica gel using hexane/CH_2Cl_2 (v : v 10 : 1) as eluent. Recrystallization from a hot mixed solvent of hexane/CH_2Cl_2 (v/v, 3 : 1) gave **D-2** (988 mg, 94%). ^{1}H NMR (400 MHz, $CDCl_3$): δ (ppm) 8.13 (4H, s, Ar–H), 7.68 (4H, d, 8.5 Hz, Ar–H), 7.55 (4H, d, 8.5 Hz, Ar–H), 7.45 (8H, m, Ar–H), 7.36 (8H, m, Ar–H), 3.8–2.0 (10H, br, B–H), 1.45 (36H, s, CH_3); ^{13}C NMR (101 MHz, $CDCl_3$): δ (ppm) 143.30, 138.75, 138.61, 133.09, 131.46, 130.61, 130.34, 126.34, 125.45, 123.73, 123.62, 120.77, 116.31, 109.14 (48C, Ar–C), 91.60, 88.54 (4C, C$\equiv$C), 84.83 (2C, C_{carb}), 34.73 (4C, CMe_3), 31.96 (12C, CH_3); ^{11}B NMR (128 MHz, $CDCl_3$): δ (ppm) −1.99 (4B, br), −9.97 (6B, br); MS (MALDI-TOF): *m*/*z* calcd for $C_{70}H_{74}B_{10}N_2$ 1051.682, found for $C_{70}H_{74}B_{10}N_2$ 1051.676; HRMS (TOF-MS ES): *m*/*z* calcd for $C_{70}H_{74}B_{10}N_2$ 1051.6783, found for $C_{70}H_{74}B_{10}N_2$ 1051.6782. Anal. calcd for $C_{70}H_{74}B_{10}N_2$: C, 79.96; H, 7.09; N, 2.66. Found: C, 79.70; H, 7.37; N, 2.34.

The synthesis of **M-3** followed that of **M-2**, but employed (4-iodophenyl)-*o*-carborane (347 mg, 1.0 mmol), 3,6-di-*tert*-butyl-9-(4-((4-ethynylphenyl)ethynyl)phenyl)-9*H*-carbazole (480 mg, 1.0 mmol), $Pd(PPh_3)_4$ (35 mg, 0.03 mmol), and CuI (10 mg, 0.05 mmol). **M-3** was obtained by recrystallization from a hot hexane/CH_2Cl_2 (v/v, 3 : 1) solution (574 mg, 82%). ^{1}H NMR (400 MHz, $CDCl_3$): δ (ppm) 8.14 (2H, s, Ar–H), 7.73 (2H, d, 8.5 Hz, Ar–H), 7.56 (2H, d, 8.5 Hz, Ar–H), 7.55–7.35 (12H, m, Ar–H), 3.91 (1H, s, C_{carb}–H), 1.46 (18H, s, CH_3); ^{13}C NMR (101 MHz, $CDCl_3$): δ (ppm) 143.27, 138.80, 138.39, 133.25, 133.06, 131.82, 131.69, 131.63, 127.60, 126.37, 125.03, 123.74, 123.60, 123.53, 122.49, 121.20, 116.32, 109.18 (30C, Ph), 91.57, 91.06, 89.65, 89.60 (4C, C$\equiv$C), 75.92 (C_{carb}), 60.06 (C_{carb}), 34.74 (2C, CMe_3), 31.98 (6C, CH_3); ^{11}B NMR (128 MHz, $CDCl_3$): δ (ppm) −1.26 (1B), −2.44 (1B), −8.17 (2B), −9.39 (2B), −10.07 (2B), −11.36 (2B); MS (MALDI-TOF): *m*/*z* calcd for $C_{44}H_{47}B_{10}N$ 698.468 (100%), found for $C_{44}H_{47}B_{10}N$ 698.465 (100%); HRMS (EI): *m*/*z* calcd for $C_{44}H_{47}B_{10}N$ 698.4561, found for $C_{44}H_{47}B_{10}N$ 698.4539. Anal. calcd for $C_{44}H_{47}B_{10}N$: C, 75.71; H, 6.79; N, 2.01. Found: C, 75.45; H, 6.44; N, 1.85.

The synthesis of **D-3** followed that of **D-2**, but employed bis(4-iodophenyl)-*o*-carborane (548 mg, 1.0 mmol), 3,6-di-*tert*-butyl-9-(4-((4-ethynylphenyl)ethynyl)phenyl)-9*H*-carbazole (959 mg, 2.0 mmol), $Pd(PPh_3)_4$ (69 mg, 0.06 mmol), and CuI (12 mg, 0.06 mmol). **D-3** was obtained by recrystallization from a hot hexane/CH_2Cl_2 (v/v, 3 : 1) solution (995 mg, 80%). ^{1}H NMR (400 MHz, $CDCl_3$): δ (ppm) 8.13 (4H, s, Ar–H), 7.72 (4H, d, 8.5 Hz, Ar–H), 7.56 (4H, d, 8.5 Hz, Ar–H), 7.54–7.30 (24H, m, Ar–H), 3.90–1.90 (10H, br, B–H), 1.46 (36H, s, CH_3); ^{13}C NMR (101 MHz, $CDCl_3$): δ (ppm) 143.28, 138.84, 138.43, 133.05, 131.64, 131.62, 131.44, 130.59, 130.41, 126.39, 125.36, 123.73, 123.63, 123.54, 122.46, 121.22, 116.31, 109.18 (60C, Ar–C), 91.82, 91.06, 89.74, 89.64 (8C, C$\equiv$C), 84.81 (2C, C_{carb}), 34.74 (4C, CMe_3), 31.98 (12C, CH_3); ^{11}B NMR (128 MHz, $CDCl_3$): δ (ppm) −2.59 (5B, br), −9.74 (5B, br); MS (MALDI-TOF): *m*/*z* calcd for $C_{86}H_{82}B_{10}N_2$ 1251.730 (100%), found for $C_{86}H_{82}B_{10}N_2$ 1251.730 (100%); HRMS (ES): *m*/*z* calcd for $C_{86}H_{82}B_{10}N_2$ 1251.7330 found for $C_{86}H_{82}B_{10}N_2$ 1251.7345. Anal. calcd for $C_{86}H_{82}B_{10}N_2$: C, 82.52; H, 6.60; N, 2.24. Found: C, 82.77; H, 6.54; N, 2.09.

Theoretical calculations

Density functional theory (DFT) computations were carried out with the Gaussian 09 package.[21] Ground state geometries were fully optimized with the M06-2X functional using the 6-31G(d,p) basis set for all atoms. The excitation energies and oscillator strengths for the lowest 5 singlet–singlet transitions from the ground state optimized geometry were obtained by time-dependent (TD)-DFT calculations also using the M06-2X functional and the 6-31G(d,p) basis set. Selected geometries of **D-1**, **D-2**, and **M-3** at their first singlet excited state were optimized at the TD-DFT level using uM06-2X/6-31G(d,P), followed by frequency analysis to verify the absence of any imaginary frequency. Emission data was obtained from the excited-state calculations without considering solvent effects. The orbital composition analysis showing the contribution of the carborane cluster was performed by Mulliken partitioning using the Multiwfn program.[22] To simplify the calculations, model compounds omitted the two *tert*-butyl groups except for **D-1**, which retained one *tert*-butyl group on each carbazole unit.

Acknowledgements

We thank the Program of Introducing Talents of Discipline to Universities (111 Project B13025), the Fundamental Research Funds for the Central Universities (JUSRP11423), the Natural Science Foundation of Jiangsu Province, China (No. BK20140140), the National Natural Science Foundation of China (No. 21502072), and the Australian Research Council for support.

Notes and references

1 (*a*) Y. Lin, Y. Li and X. Zhan, *Chem. Soc. Rev.*, 2012, **41**, 4245; (*b*) G. Bottari, G. de la Torre, D. M. Guldi and T. Torres, *Chem. Rev.*, 2010, **110**, 6768; (*c*) B. P. Rand, J. Genoe, P. Heremans and J. Poortmans, *Prog. Photovoltaics*, 2007, **15**, 659.

2 (*a*) F. Laquai, Y.-S. Park, J.-J. Kim and T. Basche, *Macromol. Rapid Commun.*, 2009, **30**, 1203; (*b*) D. M. Guldi, B. M. Illescas, C. Ma Atienza, M. Wielopolskia and N. Martin, *Chem. Soc. Rev.*, 2009, **38**, 1587; (*c*) Y. Tao, K. Yuan, T. Chen, P. Xu, H. Li, R. Chen, C. Zheng, L. Zhang and W. Huang, *Adv. Mater.*, 2014, **26**, 7931; (*d*) Q. Zhang, B. Li, S. Huang, H. Nomura, H. Tanaka and C. Adachi, *Nat. Photonics*, 2014, **8**, 326–332; (*e*) H. Uoyama, K. Goushi, K. Shizu, H. Nomura and C. Adachi, *Nature*, 2012, **492**, 234; (*f*) Z. An, C. Zheng, Y. Tao, R. Chen, H. Shi, T. Chen, Z. Wang, H. Li, R. Deng, X. Liu and W. Huang, *Nat. Mater.*, 2015, **14**, 685; (*g*) N. S. Hosmane, *Boron Science: New technologies and Applications*, CRC Press, Boca Raton, FL, 2011.

3 (*a*) S. V. Rosokha and J. K. Kochi, *Acc. Chem. Res.*, 2008, **41**, 641; (*b*) M. Gonzalez, J. L. Segura, C. Seoane, N. Martin, J. Garin, J. Orduna, R. Alcala, B. Villacampa, V. Hernandez and J. T. L. Navarrete, *J. Org. Chem.*, 2001, **66**, 8872.

4 (*a*) M. F. Hawthorne, J. I. Zink, J. M. Skelton, M. J. Bayer, C. Liu, E. Livshits, R. Baer and D. Neuhauser, *Science*, 2004, **303**, 1849; (*b*) A. M. Spokoyny, C. W. Machan, D. J. Clingerman, M. S. Rosen, M. J. Wiester, R. D. Kennedy, C. L. Stern, A. A. Sarjeant and C. A. Mirkin, *Nat. Chem.*, 2011, **3**, 590; (*c*) M. F. Hawthorne and A. Maderna, *Chem. Rev.*, 1999, **99**, 3421; (*d*) A. F. Armstrong and J. F. Valliant, *Dalton Trans.*, 2007, 4240, DOI: 10.1039/b709843j; (*e*) A. M. Spokoyny, T. C. Li, O. K. Farha, C. W. Machan, C. She, C. L. Stern, T. J. Marks, J. T. Hupp and C. A. Mirkin, *Angew. Chem., Int. Ed.*, 2010, **49**, 5339; (*f*) I. B. Sivaev and V. V. Bregadze, *Eur. J. Inorg. Chem.*, 2009, 1433, DOI: 10.1002/ejic.200900003; (*g*) K. Tanaka and Y. Chujo, *Macromol. Rapid Commun.*, 2012, **33**, 1235; (*h*) J. A. Christie, R. P. Forrest, S. A. Corcelli, N. A. Wasio, R. C. Quardokus, R. Brown, S. A. Kandel, Y. Lu, C. S. Lent and K. W. Henderson, *Angew. Chem., Int. Ed.*, 2015, **54**, 15448; (*i*) R. N. Grimes, *Carboranes*, Academic Press, New York, 2nd edn, 2011; (*j*) M. F. Hawthorne and Z. P. Zheng, *Acc. Chem. Res.*, 1997, **30**, 267; (*k*) X. Li, H. Yan and Q. Zhao, *Chem. – Eur. J.*, 2016, **22**, 1888.

5 M. Scholz and E. Hey-Hawkins, *Chem. Rev.*, 2011, **111**, 7035.

6 (*a*) B. P. Dash, R. Satapathy, J. A. Maguire and N. S. Hosmane, *New J. Chem.*, 2011, **35**, 1955; (*b*) R. N. Grimes, *Dalton Trans.*, 2015, **44**, 5939.

7 (*a*) S.-Y. Kim, Y.-J. Cho, G. F. Jin, W.-S. Han, H.-J. Son, D. W. Cho and S. O. Kang, *Phys. Chem. Chem. Phys.*, 2015, **17**, 15679; (*b*) K.-R. Wee, Y.-J. Cho, J. K. Song and S. O. Kang, *Angew. Chem., Int. Ed.*, 2013, **52**, 9682; (*c*) S. Mukherjee and P. Thilagar, *Chem. Commun.*, 2016, **52**, 1070; (*d*) A. Ferrer-Ugalde, A. Gonzalez-Campo, C. Vinas, J. Rodriguez-Romero, R. Santillan, N. Farfan, R. Sillanpaa, A. Sousa-Pedrares, R. Nunez and F. Teixidor, *Chem. – Eur. J.*, 2014, **20**, 9940; (*e*) A. Ferrer-Ugalde, E. Jose Juarez-Perez, F. Teixidor, C. Vinas, R. Sillanpaa, E. Perez-Inestrosa and R. Nunez, *Chem. – Eur. J.*, 2012, **18**, 544; (*f*) L. Weber, J. Kahlert, R. Brockhinke, L. Boehling, J. Halama, A. Brockhinke, H.-G. Stammler, B. Neumann, C. Nervi, R. A. Harder and M. A. Fox, *Dalton Trans.*, 2013, **42**, 10982; (*g*) L. Weber, J. Kahlert, R. Brockhinke, L. Boehling, A. Brockhinke, H.-G. Stammler, B. Neumann, R. A. Harder and M. A. Fox, *Chem. – Eur. J.*, 2012, **18**, 8347; (*h*) J. Kahlert, L. Boehling, A. Brockhinke, H.-G. Stammler, B. Neumann, L. M. Rendina, P. J. Low, L. Weber and M. A. Fox, *Dalton Trans.*, 2015, **44**, 9766. For dyads centered on small boron molecules, see: (*i*) C. D. Entwistle and T. B. Marder, *Angew. Chem., Int. Ed.*, 2002, **41**, 2927; (*j*) M. Elbing and G. C. Bazan, *Angew. Chem., Int. Ed.*, 2008, **47**, 834; (*k*) C.-H. Zhao, A. Wakamiya, Y. Inukai and S. Yamaguchi, *J. Am. Chem. Soc.*, 2006, **128**, 15934; (*l*) K. Suzuki, S. Kubo, K. Shizu, T. Fukushima, A. Wakamiya, Y. Murata, C. Adachi and H. Kaji, *Angew. Chem., Int. Ed.*, 2015, **54**, 15231; (*m*) Z. M. Hudson and S. Wang, *Acc. Chem. Res.*, 2009, **42**, 1584; (*n*) F. Jaekle, *Chem. Rev.*, 2010, **110**, 3985; (*o*) A. G. Bonn and O. S. Wenger, *J. Org. Chem.*, 2015, **80**, 4097.

8 (*a*) K. Kokado and Y. Chujo, *Dalton Trans.*, 2011, **40**, 1919; (*b*) K. Kokado and Y. Chujo, *J. Org. Chem.*, 2011, **76**, 316; (*c*) M. Tominaga, H. Naito, Y. Morisaki and Y. Chujo, *New J. Chem.*, 2014, **38**, 5686.

9 H. Naito, Y. Morisaki and Y. Chujo, *Angew. Chem., Int. Ed.*, 2015, **54**, 5084.

10 R. Furue, T. Nishimoto, I. S. Park, J. Lee and T. Yasuda, *Angew. Chem., Int. Ed.*, 2016, DOI: 10.1002/anie.201603232.

11 (*a*) S.-Y. Kim, A.-R. Lee, G. F. Jin, Y.-J. Cho, H.-J. Son, W.-S. Han and S. O. Kang, *J. Org. Chem.*, 2015, **80**, 4573; (*b*) B. P. Dash, R. Satapathy, E. R. Gaillard, J. A. Maguire and N. S. Hosmane, *J. Am. Chem. Soc.*, 2010, **132**, 6578.

12 A. Arrigo, A. Santoro, F. Puntoriero, P. P. Laine and S. Campagna, *Coord. Chem. Rev.*, 2015, **304**, 109.

13 (*a*) K.-R. Wee, W.-S. Han, D. W. Cho, S. Kwon, C. Pac and S. O. Kang, *Angew. Chem., Int. Ed.*, 2012, **51**, 2677; (*b*) S. Kwon, K.-R. Wee, Y.-J. Cho and S. O. Kang, *Chem. – Eur. J.*, 2014, **20**, 5953–5960.

14 A. J. Welch, *Chem. Commun.*, 2013, **49**, 3615.

15 G. F. Jin, Y.-J. Cho, K.-R. Wee, S. A. Hong, I.-H. Suh, H.-J. Son, J.-D. Lee, W.-S. Han, D. W. Cho and S. O. Kang, *Dalton Trans.*, 2015, **44**, 2780.

16 Y. Zhao and D. G. Truhlar, *Theor. Chem. Acc.*, 2008, **120**, 215.

17 (*a*) M. A. Fox, C. Nervi, A. Crivello and P. J. Low, *Chem. Commun.*, 2007, 2372; (*b*) J. Kahlert, H. G. Stammler, B. Neumann, R. A. Harder, L. Weber and M. A. Fox, *Angew. Chem., Int. Ed.*, 2014, **53**, 3702.

18 (*a*) Y. Liu, M. Nishiura, Y. Wang and Z. M. Hou, *J. Am. Chem. Soc.*, 2006, **128**, 5592; (*b*) R. M. Adhikari and D. C. Neckers, *J. Phys. Chem. A*, 2009, **113**, 417; (*c*) M. A. Fox, J. A. K. Howard, J. A. H. MacBride, A. Mackinnon and K. Wade, *J. Organomet. Chem.*, 2003, **680**, 155.

19 (*a*) H. J. Bae, H. Kim, K. M. Lee, T. Kim, Y. S. Lee, Y. Do and M. H. Lee, *Dalton Trans.*, 2014, **43**, 4978; (*b*) Y. H. Lee, J. Park, S.-J. Jo, M. Kim, J. Lee, S. U. Lee and M. H. Lee, *Chem. – Eur. J.*, 2015, **21**, 2052; (*c*) H. J. Bae, J. Chung, H. Kim, J. Park, K. M. Lee, T.-W. Koh, Y. S. Lee, S. Yoo, Y. Do and M. H. Lee, *Inorg. Chem.*, 2014, **53**, 128.

20 (*a*) A. S. Guram, R. A. Rennels and S. L. Buchwald, *Angew. Chem., Int. Ed.*, 1995, **34**, 1348; (*b*) J. Louie and J. F. Hartwig, *Tetrahedron Lett.*, 1995, **36**, 3609.

21 M. J. Frisch, G. W. Trucks, H. B. Schlegel, G. E. Scuseria, M. A. Robb, J. R. Cheeseman, G. Scalmani, V. Barone, B. Mennucci, G. A. Petersson, H. Nakatsuji, M. Caricato, X. Li, H. P. Hratchian, A. F. Izmaylov, J. Bloino, G. Zheng, J. L. Sonnenberg, M. Hada, M. Ehara, K. Toyota, R. Fukuda, J. Hasegawa, M. Ishida, T. Nakajima, Y. Honda, O. Kitao, H. Nakai, T. Vreven, J. A. Montgomery, Jr., J. E. Peralta, F. Ogliaro, M. Bearpark, J. J. Heyd, E. Brothers, K. N. Kudin, V. N. Staroverov, T. Keith, R. Kobayashi, J. Normand,

K. Raghavachari, A. Rendell, J. C. Burant, S. S. Iyengar, J. Tomasi, M. Cossi, N. Rega, J. M. Millam, M. Klene, J. E. Knox, J. B. Cross, V. Bakken, C. Adamo, J. Jaramillo, R. Gomperts, R. E. Stratmann, O. Yazyev, A. J. Austin, R. Cammi, C. Pomelli, J. W. Ochterski, R. L. Martin, K. Morokuma, V. G. Zakrzewski, G. A. Voth, P. Salvador, J. J. Dannenberg, S. Dapprich, A. D. Daniels, O. Farkas, J. B. Foresman, J. V. Ortiz, J. Cioslowski and D. J. Fox, *Gaussian 09, Revision B.01*, Gaussian, Inc., Wallingford CT, 2010.

22 (*a*) T. Lu and F. Chen, *J. Comput. Chem.*, 2012, **33**, 580; (*b*) T. Lu and F. Chen, *Acta Chim. Sin.*, 2011, **69**, 2393.

